Journal of Gastroenterology and Hepatology

JGHF

doi:10.1111/jgh.14721

HEPATOLOGY

Human liver regeneration following massive hepatic necrosis: Two distinct patterns

Katalin Dezső, Péter Nagy and Sándor Paku

First Department of Pathology and Experimental Cancer Research, Semmelweis University, Budapest, Hungary

Key words
3D reconstruction, α-fetoprotein, foci, fulminant liver failure, portal vein.

Accepted for publication 7 May 2019.

Correspondence
Sándor Paku, First Department of Pathology and Experimental Cancer Research, Semmelweis University, Üllői Street 26, 1085 Budapest, Hungary.
Email: paku@korb1.sote.hu

Declaration of conflict of interest: We have nothing to declare.
Financial support: This work is supported by TÁMOP 4.2.4.A/1-11-1-2012-0001 "National Excellence Program" and János Bolyai Scholarship of the Hungarian Academy of Sciences and Hungarian National Research, Development and Innovation Office (grants NVKP_16-1-2016-0004 and NFKIH 116301).

Abstract

Background and Aim: Massive hepatic necrosis is a rare but often fatal complication of various liver injuries. Nevertheless, some patients can survive by spontaneous hepatic regeneration. It is known that surviving hepatocytes and/or progenitor cells can participate in this process but the mechanism of hepatic recovery is vague.
Methods: We examined 13 explanted human livers removed for acute liver failure. Combined immunohistochemistry, digital image analysis, and three-dimensional reconstruction of serial sections were applied.
Results: Two patterns of regeneration could be distinguished. In livers with centrilobular necrosis, the surviving injured periportal hepatocytes started to proliferate and arrange into acinar structures and expressed α-fetoprotein. If the injury wiped out almost all hepatocytes, large areas of parenchymal loss were invaded by an intense ductular reaction. The cells at the distal pole of the ductules differentiated into hepatocytes and formed foci organized by the branches of the portal vein. The expanding foci often containing complete portal triads were arranged around surviving central veins. Their fusion eventually could be an attempt to re-establish the hepatic lobules.
Conclusions: Regeneration of human livers following massive hepatic necrosis can occur in two ways—either through proliferation of α-fetoprotein-positive acinary-arranged hepatocytes or through ductular progenitor cells, with the latter being less efficient. Further investigation of these regenerative pathways may help identify biomarkers for likelihood of complete regeneration and hence have therapeutic implications.

Introduction

Massive hepatic necrosis (MHN) with consequent fulminant liver failure is a rare but very severe complication of liver disease with various etiology.[1] Although this condition often results in the death of the patients, 10–20% of them can recover spontaneously, without liver transplantation. Surprisingly, the normal liver architecture can be restored in these survivors underlining the exceptional regenerative capacity of the liver. Unfortunately, no reliable markers exist that can predict who will be able to recover,[2] and our knowledge on the mechanism of the regeneration following MHN is also quite limited.

The largest group of patients dying of fulminant hepatic failure was described by Lucké[3] and Lucké and Mallory[4] who reviewed the major autopsy findings of American soldiers with "fatal hepatitis." They provided very comprehensive histological characterization of the events by traditional histological stainings

The destructive change (necrosis) began in the central part of the lobule. The obliteration preferentially affected the hepatocytes, while sinusoidal framework of the liver remained intact. Regenerative hyperplasia was observed in the parenchyma that had escaped destruction. In addition, "proliferative bile ducts" were frequently seen, which often had close relationships with hepatocytes. Neither the expansion of the lesions nor the degree of regeneration correlated with the duration of the disease.

Later studies applying ancillary techniques also supported that MHN was followed by regenerative changes in the surviving hepatocytes and that proliferating ductules, nowadays referred to as "ductular reaction,"[5–12] were also present. Although it has been recently questioned, in the last decades, the ductular reaction was thought to be a progenitor cell-driven regenerative process. The ductular reaction always emanated from the periportal zone, and its intensity was often found to be correlating with the extent of parenchymal damage. The ductular cells expressed biliary-type cytokeratins (CK7/19), but focal expression of hepatocytic markers (HepPar1, AAT, and HNF4) was also often observed. These results suggested that the ductular reaction represented a cell population arising from progenitor cells and played an important role in regeneration. This notion was nicely supported by sequential biopsies of the native liver of a patient, whose MHN was treated by auxiliary liver transplantation.[10] The intensity of ductular reaction gradually increased, after which round clusters of hepatocyte like cells were formed, and finally, the trabecular pattern of hepatic parenchyma was re-established. Regenerative clusters[13] and regenerative nodules[14–16] of hepatocytes following MHN have not been thoroughly investigated but were briefly mentioned in other reports.

We have been systematically analyzing the architectural aspects of various hepatic regenerative processes.[17–19] Regardless of the cellular origin (hepatocytes or ductular cells), the basic lobular structure is maintained or eventually re-established during liver regeneration. If this process is impeded by extensive scarring, the derailed regeneration results in liver cirrhosis.[19] However, the formation of cirrhotic nodules is also a highly coordinated process organized by the pre-existent branches of the portal vein.

Oval cells in ductular arrangement differentiated into "small hepatocytes" forming foci supplied by branches of the portal vein in several experimental liver regeneration models.[18] The components of this process (ductular reaction, hepatocyte foci, and recovery of lobular structure) showed striking similarities with the alterations described in human livers following MHN.

We were curious if any "regenerative pattern" could be observed in human livers removed from patients at the time of orthotopic liver transplantation due to MHN. We were able to gather histological blocks from our archives, but the available material was limited, and naturally, we had only one "observation time point" from each patient. Yet by applying the techniques of combined immunohistochemistry, digital image analysis, and three-dimensional reconstruction of serial sections, we were able to distinguish two types of regeneration and recognize similarities with previously described regenerative mechanisms.[20]

Methods

Human liver samples. Retrospective analysis of 13 explanted livers with acute/subacute liver failure of different etiologies was performed. Clinical data of the patients, the etiology of liver failure, and the time elapsed between appearance of clinical symptoms and liver transplantation is summarized in Table S1.

The study protocol was approved by the Ethical Commission of Semmelweis University (no. 125/2010).

Results

In this retrospective study, we analyzed tissue samples of 13 explanted livers removed because of acute liver failure. Based exclusively on the morphological pattern of standard histological and immunohistochemical staining, blindly to the clinical data, the livers could be stratified into four groups:

1 Two cases were characterized by large central necrosis (Fig. 1a), accompanied by mild ductular reaction, which was obvious only by CK19 immunostaining (Fig. 1b). These ductules were elongated tortuous biliary channels. They terminated in a "spiky" or "U-shaped" end on a hepatocyte, like the canals of Hering in normal hepatic tissue.

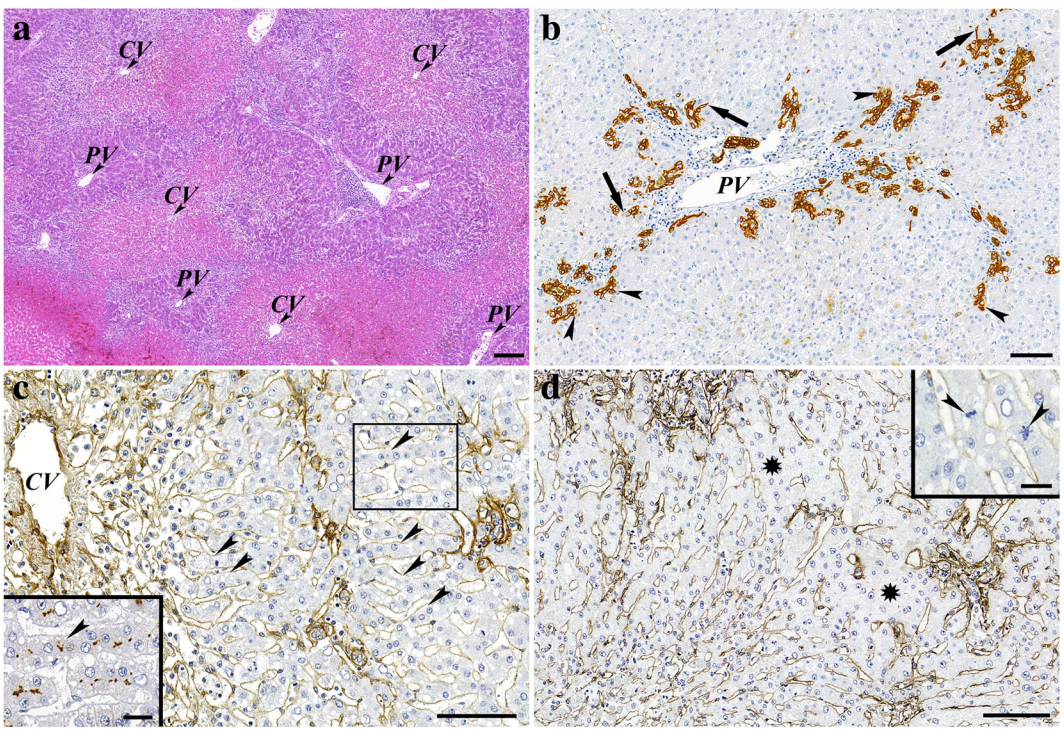

Figure 1 Group 1 livers with centrilobular necrosis. (a) On the hematoxylin and eosin-stained section, the confluent necrotic areas are discernible. Periportally intact parenchyma is present. (b) Around the portal vein, large number of CK19-positive bile ductules are present. A proportion of them terminate in "spiky" (arrows) or "U-shaped" (arrowheads) ends on hepatocytes. (c) Laminin staining highlights numerous one-cell-thick hepatic plates (arrowheads), which are oriented toward the central vein. Around the central vein, the liver parenchyma is collapsed, but the skeleton of sinusoids is still discernible. The inset shows at higher magnification the boxed area stained for CD10 on an adjacent section. The staining demonstrates the normal organization of the bile canaliculi (dots or lines between adjacent hepatocytes) within the hepatic plates. (d) Laminin staining shows widened hepatic plates (asterisks) periportally. The inset shows hepatocytes in mitosis (arrowheads). Scale bar: (a) 200 μm; (b) 100 μm; (c) 100 μm (inset: 20 μm); and (d) 100 μm (inset: 20 μm). *CV*, central vein; *PV*, portal vein.

Their immunophenotype was also identical with normal biliary structures; no signs of hepatocytic differentiation could be observed. The periportal parenchyma was constructed by almost undisturbed one-cell-thick to two-cell-thick hepatic plates (Fig. 1c), although occasional dividing hepatocytes were observed, resulting in the widening of the liver plates (Fig. 1d). Smooth muscle actin (SMA)-positive cells accumulated pericentrally (Fig. S1a). The collapsed supportive collagen network of the sinusoids remains preserved at this area (Fig. S1b).

2 Central or occasionally bridging necrosis was also present in six other livers. The periportal ductular reaction was similar in both architecture and immunophenotype to the one described earlier. However, substantial alterations occurred in the surviving parenchyma. The hepatocyte-like cells often formed acinar structures (CD10 positivity at the apical membrane) sometimes with a bile plug in the central lumen (Fig. 2a). These "acinar hepatocytes" were positive for hepatocytic lineage markers such as arginase-1 (Fig. 2b) but did not stain for CK19 (Fig. 2b,c) and epithelial cell

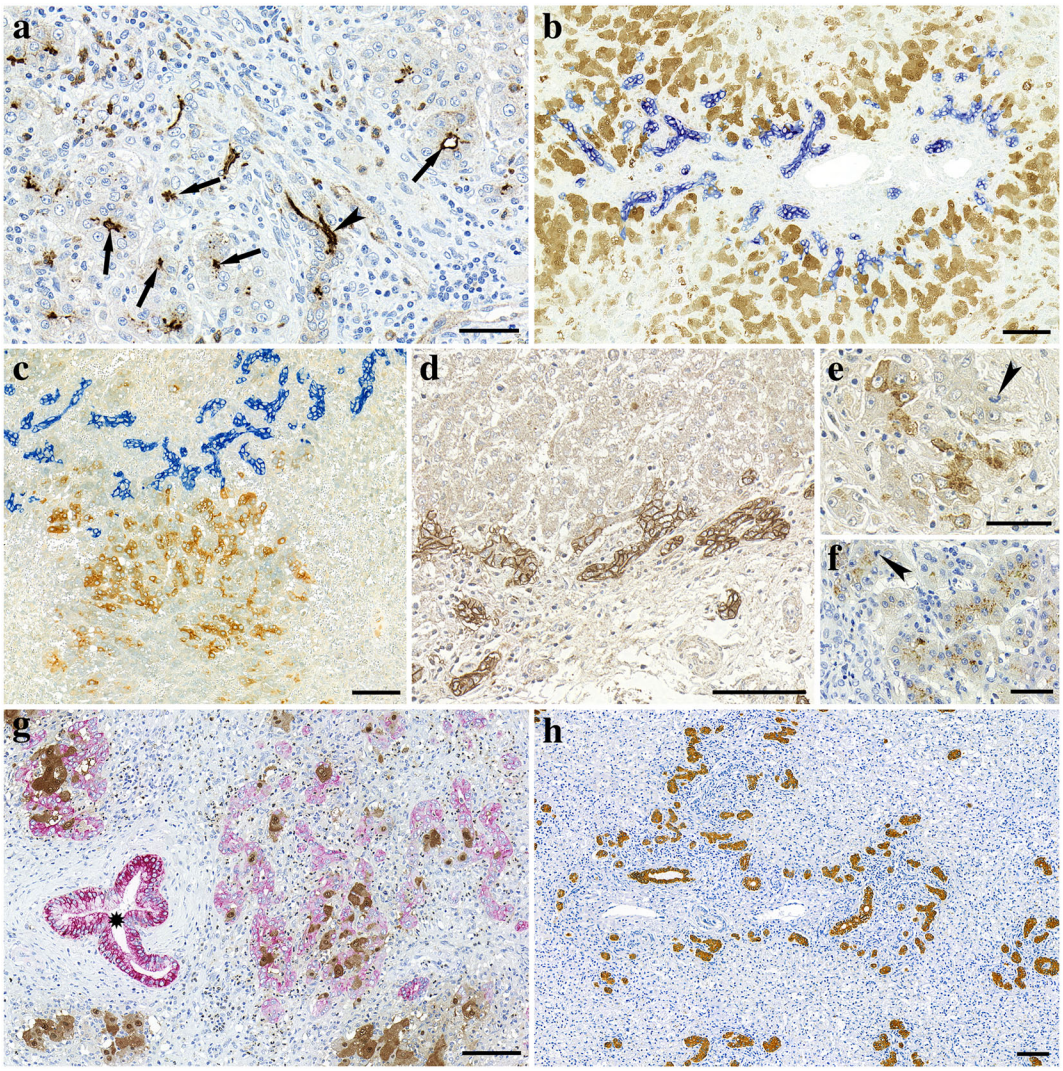

Figure 2 Group 2 livers with surviving hepatocytes (a–f) and group 3 livers with parenchymal loss (g–h). (a) CD10 staining is present at the apical pole of hepatocytes forming acinar structures (arrows). Arrowhead points at a bile duct. (b) Double labeling for arginase-1 (brown) and CK19 (blue). Surviving hepatocytes in the parenchyma are positive for arginase-1 but negative for CK19, which latter is present in the periportal bile ductules. (c) Double labeling for α-fetoprotein (AFP) (brown) and CK19 (blue). A large proportion of surviving hepatocytes is positive for AFP. AFP is not present in the CK19-positive bile ductules. (d) Bile ductules bordering the surviving parenchyma are positive for epithelial cell adhesion molecule. No specific staining is visible in the hepatocytes. (e, f) Acinary-arranged hepatocytes express DLK-1 (e) and glypican-3 (f). Arrowheads point at hepatocytes in mitosis. (g) Double labeling for arginase-1 (brown) and CK19 (red). The large bile duct (asterisk) is strongly positive for CK19 but negative for arginase-1. In contrast, the ductular reaction shows variable but diminished CK19 positivity. Within the ductular reaction, scattered arginase-1-positive hepatocyte-like cells are present. At the bottom of the picture, remnants of the original parenchyma are visible, which are not related to the ductular reaction. (h) Section stained for CK19 from a liver with complete parenchymal loss. In the absence of hepatocytes, the blind-ending ductules show rounded morphology. Scale bar: (a, e, f) 50 μm; (b, c, d, g, h) 100 μm.

adhesion molecule (EpCAM) (Fig. 2d). The most striking feature of this group was the focal positivity of hepatocytes for α-fetoprotein (AFP) (Fig. 2c), DLK-1 (Fig. 2e), and glypican-3 (Fig. 2f). AFP-positive, DLK-1-positive, and glypican-3-positive cells appeared to outline the acinar structures, but single positive hepatocytes were also observed. The stained cells had no preferential lobular distribution or morphology.

3 The next group of livers was characterized by parenchymal loss. In fact, on the sections from one of the livers, not a single parenchymal hepatocyte could be seen, while small islands of arginase-1-positive hepatocytes were present in the other one (Fig. 2g). The portal areas were highlighted by the intense radially arranged ductular reaction (Fig. 2h). The ductules were surrounded by SMA-positive myofibroblasts depositing collagen (Fig. S1c,d). There were two basic differences between the ductules in these livers and the ones seen in the two former groups. (i) While the short ductules in the groups 1 and 2 were constructed exclusively by typical cholangiocytes, occasional larger cells participated in the formation of the ductules of this group. These cells stained faintly by CK19 antibody but expressed the hepatocyte marker arginase-1 (Fig. 2g). (ii) In the absence of hepatocytes, the ductules had no contact with the hepatic plates; consequently, they had been sealed by rounded end (Fig. 2g,h).

4 The last group of livers could be distinguished by the presence of well circumscribed, usually round hepatocytic foci. No remnant of the original parenchyma was seen in these samples. The relationship of the foci to the arterioles, to the portal and central vessels, and to the ductular reaction could be determined by co-staining for CD34 and CK19. On areas with parenchymal loss (without foci), the outline of the original lobular structure was preserved and could be easily identified (Fig. 3a). The portal areas were surrounded by CK19-positive ductular reaction similarly to the ones described in group 3. The CD34 antibody stained the portal vessels and the capillaries/sinusoids meandering among the ductular reaction. These vessels were in connection with portal venules (Figs 3b,S2).

The ductules showed strong polarization in one of our specimens. The cells of distal part of ductules were larger, had eosinophil cytoplasm (Fig. 3c), and showed diminished CK19 positivity (Fig. 3d,e); reversely, expression of hepatocytic lineage markers such as arginase-1, HNF4, and CYP-450 (Fig. 3e–g) was increased. The intensity of EpCAM staining was nevertheless even along these ductules, and the differentiating cells remained positive (Fig. 3f).

On the areas of parenchymal loss foci of hepatocytes, which grew independently from each other in the early phase of their development, were formed (Fig. 4a). However, larger foci often fused with each other (Fig. 4b). The distribution of the foci was not random; they developed preferentially at the periphery (distal from the portal triad) of the ductular reaction (Fig. 4c and Movie S1).

Thorough analysis of serial sections showed that the majority of the foci were connected directly to terminal portal venules (Table S2). The smallest foci (~up to 200 μm) were connected to the portal system by capillaries/sinusoids, but terminal portal venules appeared in the center of growing foci (Fig. 4d–f). These foci did not contain bile duct(ule)s or arterioles. Draining ductules were present only at their surface (Fig. 4g–h). Arterioles and bile ducts turned up in the foci at later stage of their development (Fig. S3a–c), and the ducts frequently terminated within the foci (Table S2 and Fig. S3d).

All the examined large-sized (frequently fused) foci were connected to portal venules/veins (Table S2), and the majority (80%) of the foci contained complete portal triads in central position (Figs 5,S4). Bile ductules were not present on the surface of the foci; they could be detected inside the foci, mostly at the periphery of the incorporated portal areas.

The developing frequently fused foci containing complete portal triads surrounded central veins. This arrangement was reminiscent of a liver lobule (Figs 6,S5). However, the central veins often seemed to be compressed by the growing foci (Fig. S5).

Discussion

Detailed histological analysis was performed on the available 13 explanted liver samples removed for acute liver failure. Group 1 samples might represent the initial phase of the liver injury, which was characterized by centrilobular necrosis. We propose that two well-defined regenerative patterns can be distinguished (Fig. 7). The regeneration is completely accomplished by hepatocytes in group 2, while the hepatic progenitor cell compartment attempts to recover the liver parenchyma by means of ductular reaction and subsequent formation of hepatocyte foci in groups 3 and 4.

These processes perfectly fit to the almost dogmatically repeated paradigm that hepatocytes have an excellent regenerative capacity, but if they fail, the "backup" progenitor cell compartment, presumably located in the canals of Hering, gets activated.[20–23] This "traditional" view has recently been questioned, but eventually, lineage tracing experiments in mice supported the significant contribution of progenitor cells to the restoration of liver parenchyma.[24]

Hepatocyte-mediated regeneration. The regeneration was triggered by centrilobular or occasionally bridging necrosis in group 2. Although a mild periportal ductular reaction was present in these livers, it could be hardly recognized on hematoxylin and eosin-stained sections, and it was completely negative for hepatocyte lineage markers (arginase-1 and HNF4). At the same time, the surviving hepatocytes formed peculiar acinar structures with occasional mitoses. We certainly cannot exclude their ductular origin, but the arrangement and arginase-1 positivity along with a relatively mild ductular reaction might indicate that these are surviving hepatocytes. This notion was further supported by the lack of EpCAM staining, because this is the most accepted marker of progenitor cell-derived hepatocytes.[25] The most surprising result was the extensive positivity of these acinar hepatocytes for AFP and occasionally for DLK-1 and glypican-3. AFP is a well-established oncofetal marker highly expressed by fetal hepatoblasts and hepatocellular carcinomas.[26] The positivity of rat oval cells for AFP was a strong argument for their "stem cell" nature.[27] The increased AFP level in the serum of patients with acute liver failure[28,29] was taken as evidence for the participation of hepatic progenitor cells in regeneration. Surprisingly, most of the immunohistochemical studies (including our group's)

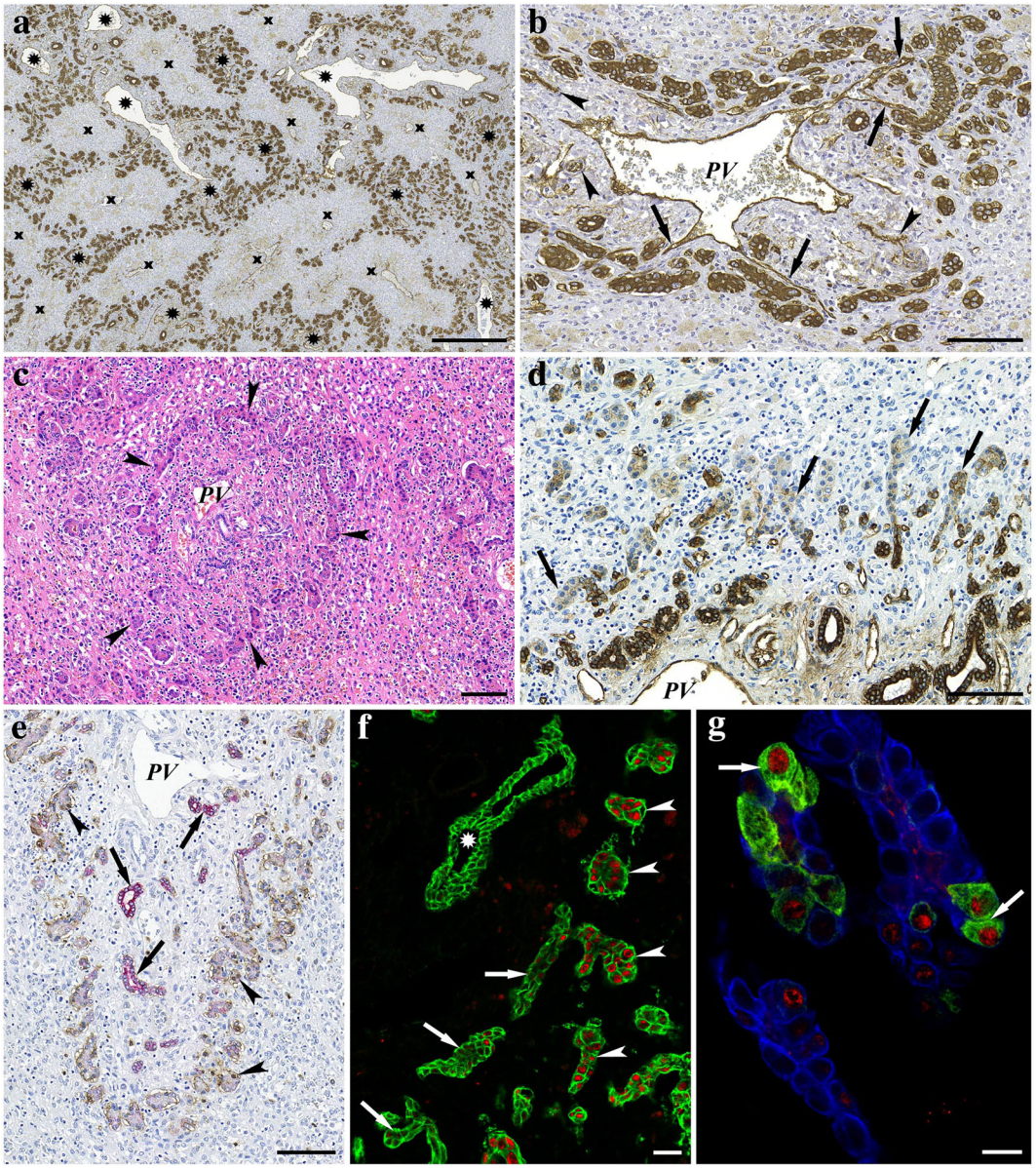

Figure 3 Group 4 livers with regenerative foci in the areas of parenchymal loss. (a) Area of parenchymal loss stained for CK19 and CD34. The skeleton of liver lobules is discernible. The portal areas are marked by asterisks; the central areas are marked by x. The central veins stained by the anti-CD34 antibody are surrounded by a halo area (the CD34 antibody does not stain the sinusoids located at this area), and extensive ductular reaction can be observed around the portal areas. (b) High-power micrograph of a portal area stained for CK19 and CD34. CD34-positive capillaries/sinusoids (arrows) that originate from the portal vein are localized close to the CK19-positive ductules. Arrowheads mark the branches of the hepatic artery. The run of the capillaries among the ductular reaction that is demonstrated on 10 serial sections shown on Figure S2, and (b) corresponds to Figure S2h. (c–g) Formalin-fixed paraffin-embedded (c–e) and frozen (f–g) sections of the liver sample with strongly polarized ductular reaction. (c) Hematoxylin and eosin-stained section of an area of parenchymal loss. The cells of the distal ring (arrowheads) of the ductules around the portal vein are enlarged and have eosinophilic cytoplasm. (d) CK19-stained section. Note the gradual loss of the CK19 positivity (arrows) along the ductules away from the portal area. (e) CK19 (red) arginase-1 (brown) double labeling. The bile ducts close to the portal vein (*PV*) are strongly positive for CK19 (arrows). The CK19 reaction is diminished in the distal part of the ductular reaction; reversely, cells of this area have gained weak cytoplasmic and occasionally strong nuclear (arrowheads) arginase-1 positivity. (f) Double labeling for epithelial cell adhesion molecule (green) and HNF4 (red). The large bile duct (asterisk) in the portal area is strongly positive for epithelial cell adhesion molecule but negative for HNF4. Some of the ducts show variable HNF4 positivity along their path (arrows). There are also ducts situated more distally with strong nuclear HNF-4 staining (arrowheads). (g) Triple labeling for CYP-450 (green), HNF4 (red), and CK19 (blue). High-power confocal image of the distal part of the ductular reaction. Ductular cells are present at variable stages of differentiation. Cells with strong CYP-450 and HNF4 positivity show weak positivity for CK19 (arrows). Scale bar: (a) 500 μm; (b–e) 100 μm; and (f–g) 20 μm.

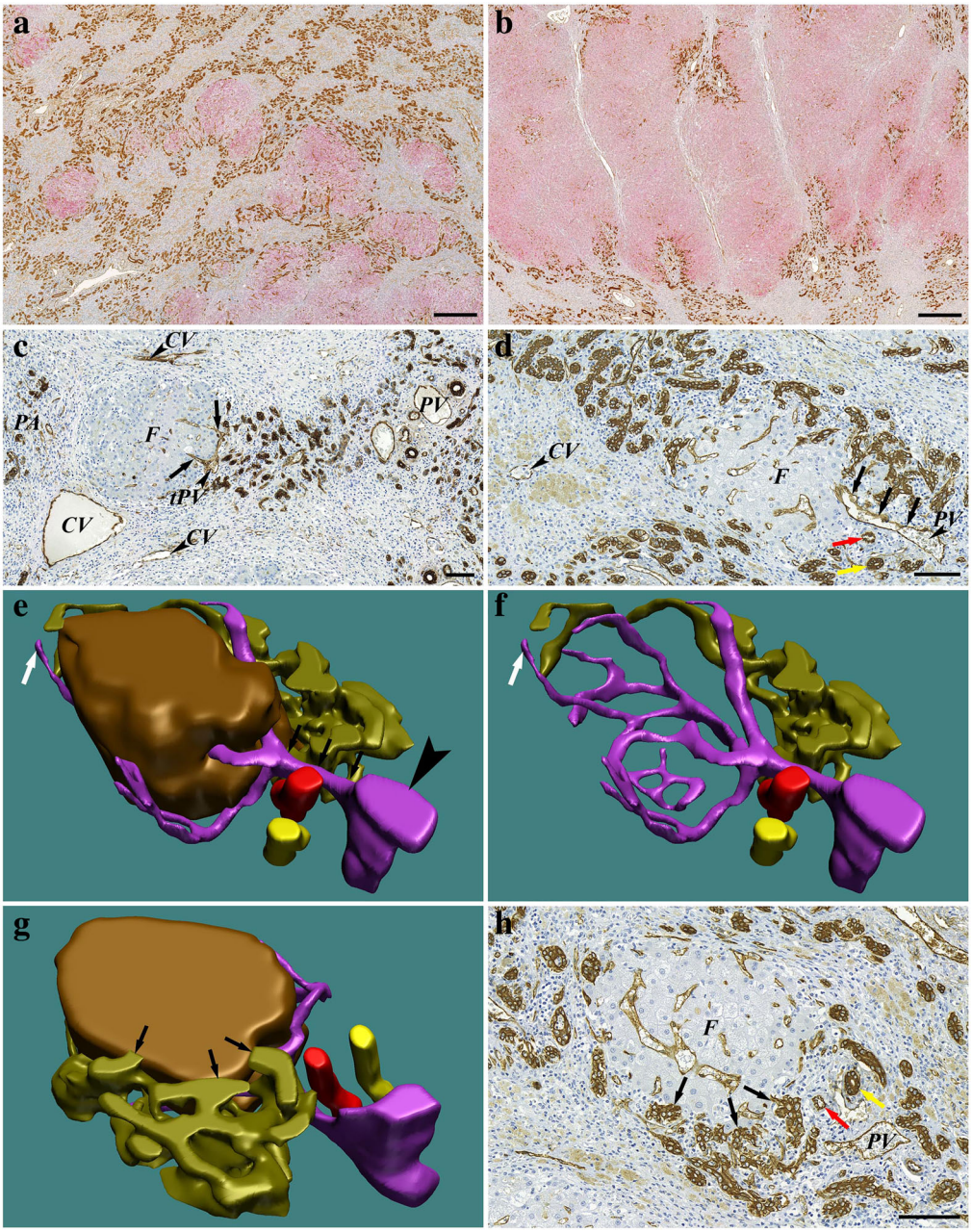

Figure 4 Architecture of the foci. (a, b) Sections of livers (different patients) from group 4 containing predominantly small-sized foci (a) or large-fused foci (b). Both sections are stained for arginase-1 (red) to highlight the foci. The sections are also stained for CK19 and CD34 (brown) to show the localization of the ductular reaction and vessels. (c) Focus (*F*) localized at distal part of the ductular reaction. The picture shows the 61st section of a series of 86 sections shown on Movie S1. The terminal portal venule (*tPV*) that originates from the portal vein on the right side of the picture (*PV*) enters the focus on this section (arrows). The run of the terminal portal venule (marked on the Movie S1) is oriented toward another portal area (*PA*). The focus is localized between central veins (*CV*). (d–h) Three-dimensional reconstruction of a small focus. (d) The localization of the focus on the area of parenchymal loss. The focus (*F*) is embedded in the ductular reaction. The terminal portal venule (black arrows, *PV*) that supplies the focus is visible on the right, whereas central vein (*CV*) is present on the left side of the picture. (e) The relationship of the focus (brown) to the portal vein (purple), artery (red), bile ducts (yellow), and ductular reaction (greenish). The terminal portal venule (black arrows, visible also on d) that supplies the focus originates at right angle form the larger branch of the portal vein (large arrowhead) running parallel to the artery and bile duct. The periphery of the focus is close to the segment of the terminal portal venule where it branches into capillaries/sinusoids. No branches of the artery or the bile duct are oriented toward or enter the focus. (f) The delicate network of vessels within the focus. The vessel marked by white arrow leaves the focus toward the central vein. (g, h) The focus at reverse angle. At the surface, numerous canals of Hering-like structures draining the focus are visible on the reconstruction (g) and on the corresponding section (h) (black arrows). Bile ductules are not present within the focus. Yellow and red arrows on (d) and (h) point at the bile duct and at the artery. Scale bar: (a, b) 500 μm; (c, d, h) 100 μm.

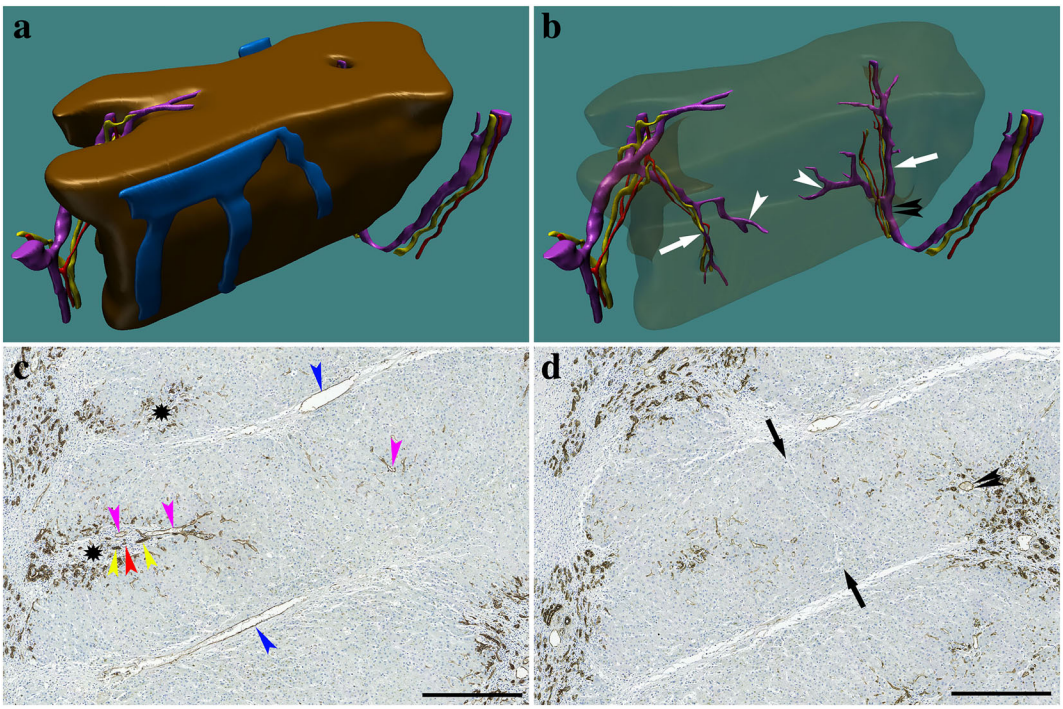

Figure 5 Architecture of the fused foci. (a–d) Three-dimensional reconstruction of fused foci (101 sections were used for the reconstruction). The foci developed around adjacent portal tracts. The reconstructed structure represents one-sixth of a regenerating liver lobule. (a, b) The relationship of the fused foci (brown) to the central veins (blue), portal veins (purple), arteries (red), and bile ducts (yellow). The central veins are located outside of the foci. In (b), complete portal triads are visible within the fused mass (white arrows). Note that the terminal segment of the portal vein is not accompanied by arteries and bile ducts (white arrowheads). (c) A section of the series (section 99) close to the top of the reconstruction. Colored arrowheads point at the corresponding structures on the reconstruction. Central veins (blue arrowheads) are located between adjacent foci, which later are not visible on the reconstruction. Note that bile ducts are not present at the outer surface of the foci; they are located inside the foci at the periphery of the portal areas (asterisks). (d) The 29th section of the series. Arrows mark the putative former border between the two fused foci. Double arrowhead points at the position of the right portal tract on the section and on the reconstruction (b). Scale bar: (c, d) 500 μm.

were not able to demonstrate AFP expression in these liver samples.[5–7,9,30] However, AFP expression was successfully demonstrated in human ductular reactions in peritumoral tissue[31] and following MHN.[14] We have no better explanation than technical failure for this inconsistency. DLK-1 is a less frequently used marker that is co-expressed with AFP in experimental animals and in human hepatoblastomas.[32] Glypican-3 is a reliable marker of hepatocellular carcinoma.[33] All of these antibodies failed to stain anything in our other experimental groups 1, 3, and 4. Our interpretation is that the AFP, DLK-1, and glypican-3 production of acinary-arranged hepatocytes might all be histomorphological signs of hepatocyte "dedifferentiation" and markers of hepatocyte-mediated regeneration in livers with MHN.

Ductular reaction-mediated regeneration. The samples classified in groups 3 and 4 may represent earlier and later stages of liver regeneration by means of the hepatic progenitor cell compartment. There were hardly any surviving hepatocytes on these livers sections, but large areas of parenchymal loss occurred. In MHN, the parenchymal cells are wiped out by viral infection, toxic damage, or other etiologies.[34] However, as already described by Lucké,[3] the sinusoidal framework of the liver was preserved. On the areas of parenchymal loss, intense periportal ductular reaction was present. These ductules were not only longer than the ones in groups 1 and 2, but also they had no connection with the hepatocytes, leading to characteristic rounded ends. In one of our samples, these ductules were extremely polarized. Small groups of enlarged cells with pale CK19 expression showed up preferentially in the distal portion of the ductules. These cells expressed hepatocytic lineage markers (arginase-1 and HNF4), but they were also positive for EpCAM. The presence of this marker, in addition to their spatial arrangement, supported their ductular origin.[25]

Isolated round clusters of hepatocytes, called foci, showed up on these areas of parenchymal loss in group 4. The foci most probably derived by budding (differentiation) from the ductular reaction. In a recent paper,[19] we demonstrated that the development of the regenerative nodules in cirrhotic livers was organized by the portal tree, that is, the regenerative nodules grew around terminal portal venules. Here, we show that following MHN, the development of individual regenerative foci is also organized by the portal tree. This supports the important role of portal blood in the induction of ductular cells' differentiation into hepatocytes. Unfortunately, it is still unknown which components of the blood[35] are responsible for boosting the differentiation. The main morphological difference between the two conditions (MHN and cirrhosis) is that the

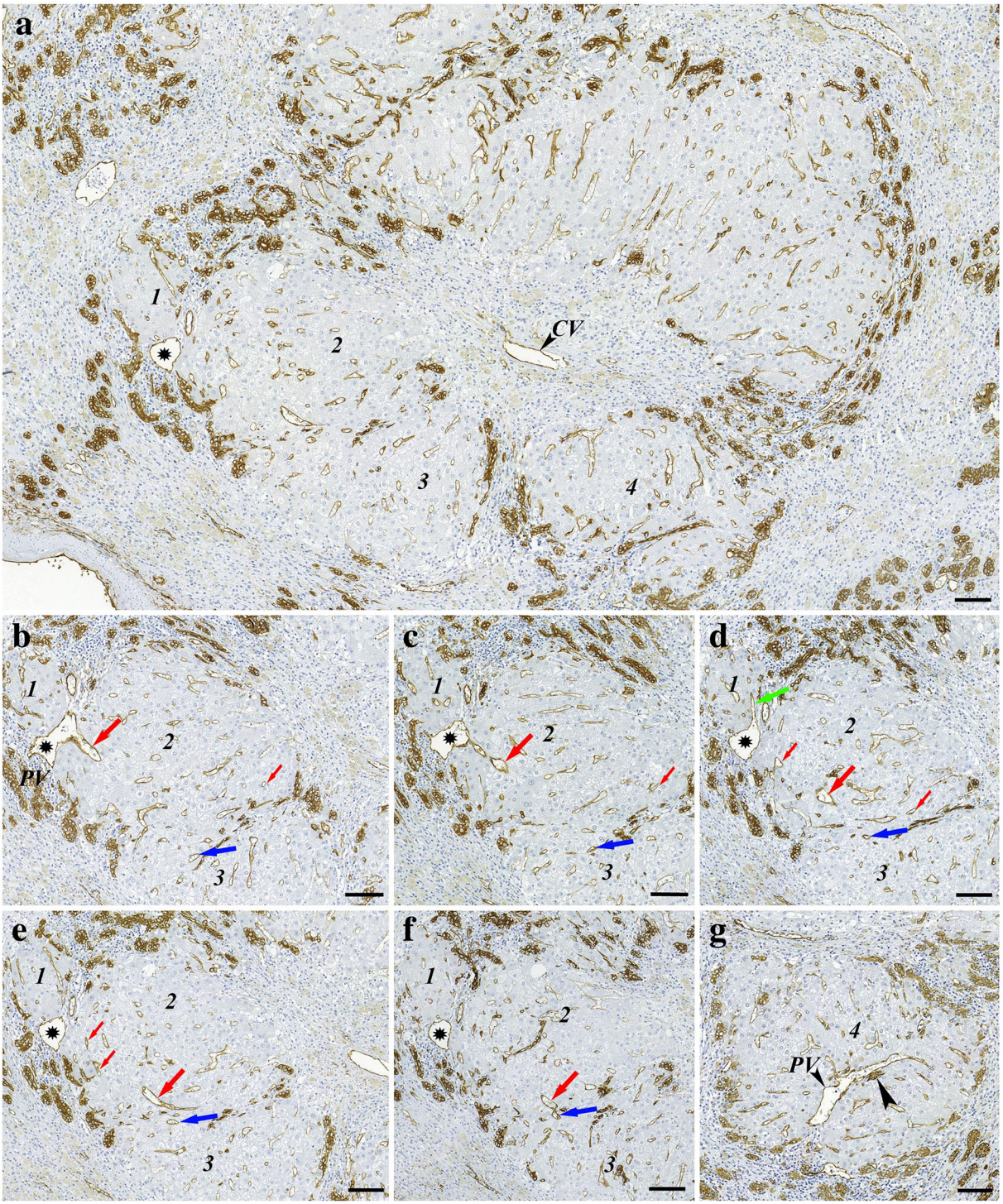

Figure 6 Regenerating liver lobule. (a) The lobule is formed around a central vein (*CV*) and can be divided into foci, which are fused with each other in different extent. Each focus has its own supplying portal vein branch. The portal vein branches supplying the foci composing the upper part of the lobule are shown on Figure S5. The lower part of the lobule can be divided into four foci (1–4). The supplying portal vein branches are shown on serial sections (b–g). Foci 1–3 are supplied by branches of a large portal vein (asterisk). A small vessel branch entering focus 1 (green arrow) on (d). Focus 3 is supplied by a vessel (blue arrows) originating from a portal vein branch, which passes through focus 2 (large red arrows on b–f). This vessel also supplies focus 2 (capillaries/sinusoids branched from this vessel marked by small red arrows). The connection between the two branches is visible on (f). Focus 4 is supplied by a different portal vein branch (*PV*) located in the center of the focus (g). This vessel is accompanied also by a bile duct (arrowhead). Arteries are not present in the foci. Scale bar: (a–g) 100 μm.

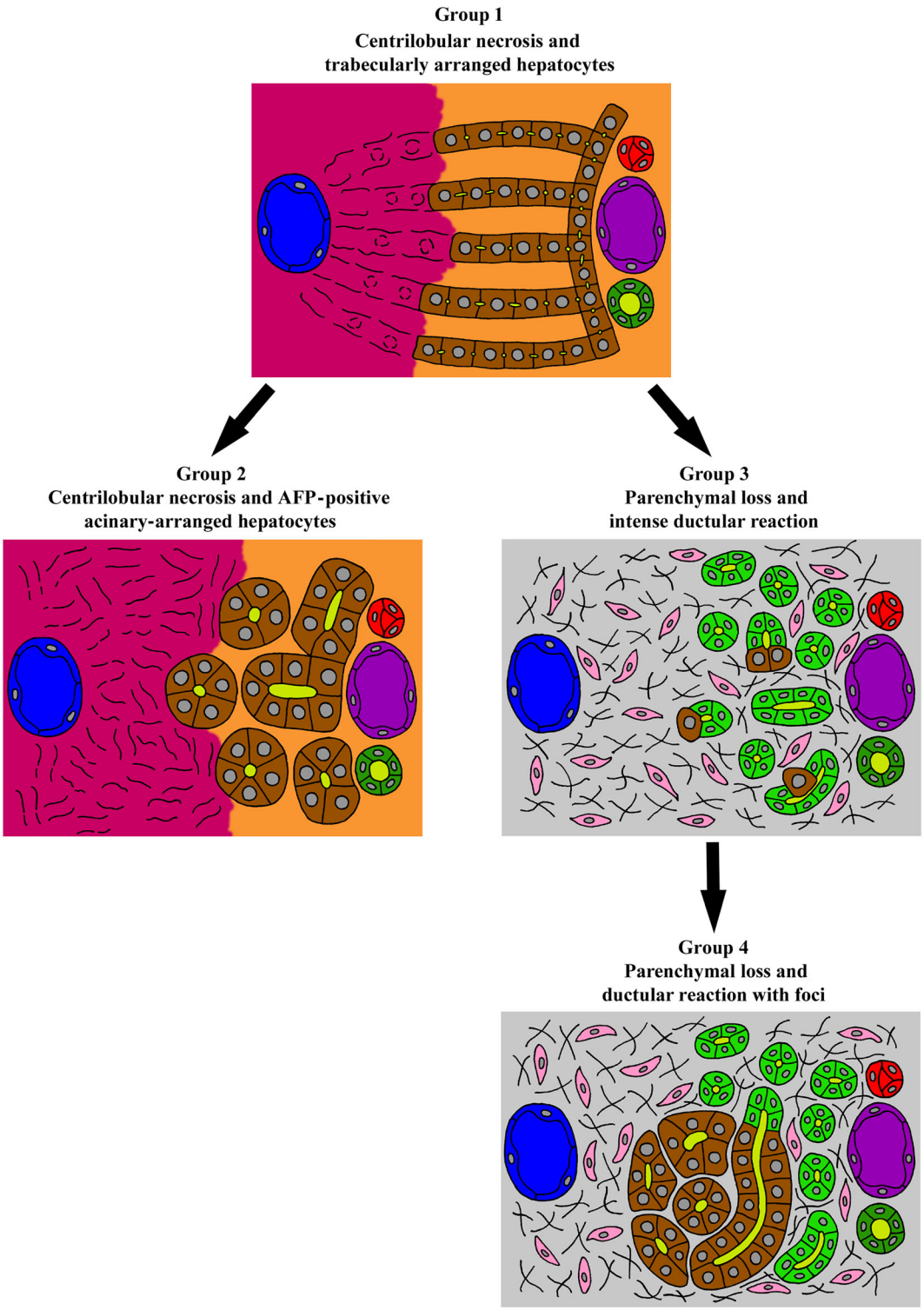

Figure 7 Schematic representation of the two regenerative patterns. , hepatocytes; , necrotic liver tissue; , surviving liver tissue; , artery; , portal vein; , central vein; , lumen of the biliary system; , interlobular bile duct; , ductular reaction; , myofibroblasts; , connective tissue.

growing foci in the former condition readily incorporate the portal triad, whereas in cirrhosis, the bile ducts and arteries are excluded from the regenerative nodules. Although signs of scarring are present on the areas of parenchymal loss (increase in the number of SMA-positive cells and in the amount of deposited collagen), the damage is probably not severe or long standing enough to

cause serious changes in the basic structure of the liver. In contrast, in cirrhotic livers, the frustrated regeneration distorts basic structural components of the liver (central veins are not recognizable; however, the portal tree is left intact). This can be the main cause of the difference observed between the structure of foci and nodules (in foci complete portal triads are present, whereas in cirrhosis, only the portal vein branches are seen, and they are separated from bile ducts and arteries).

The observed polarized differentiation of ductular cells around the intact portal tracts results in the appearance of foci in the distal region of the ductular reaction. The growing foci eventually fuse and enclose the draining bile ducts, leaving no ducts at the surface of the foci that are oriented toward either the central vein or other portal tracts. Where the differentiation of the ductular cells is less polarized, scattered groups of differentiated cells arise along the distal segment of the ductular reaction, leaving draining ductules randomly localized inside or outside the foci.

We intentionally use the term "foci" for the regenerative structures in livers with MHN (in cirrhotic livers these structures called as nodules) because these structures show a very close resemblance to the regenerative foci observed in rat livers.[18] In this model (AAF/Ph), the foci developed around the portal tracts in a liver without parenchymal loss and readily incorporated bile ductules. The foci later melted into the surrounding parenchyma. Beside the similarity between the foci structure of the human and rat liver, there is an important difference between the two regenerative processes, namely, that in the human liver, the foci develop in areas of parenchymal loss. The expansion of more foci with portal triads in their core (the foci can also fuse with each other) surrounding a central vein represents an attempt to regenerate the lobular structure of the liver. This is possible because the basic structural components of the lobules (central veins and portal tracts) are present in their original architecture at the areas of parenchymal loss.

Regeneration of the liver parenchyma by foci or nodules (expanding spheres) resulting in the compression of central veins may lead to improper circulation of the new parenchyma. This suggests that this form of regeneration may not result in a properly functioning organ.

The relation between the two patterns of regeneration. If two types of regeneration can be distinguished following MHN, it would be very important to know the relation between them and most importantly whether there is any difference between them in etiology and especially in prognosis. We could not find evidences whether the proposed two patterns of regeneration can be present in the same liver. While in the first two groups of liver, surviving parenchyma was visible, in the third group, the proportion of remaining viable liver parenchyma was negligible. In the fourth group, practically no remnant of the original parenchyma was discernible, large areas of parenchymal loss was present. There was quite a substantial variation in the extent of necrosis and areas of parenchymal loss, but the pattern of regeneration was similar. Lucké[3] also observed that the lesions were relatively uniform in all parts of the studied livers. When samples of acute liver failure were investigated by gene expression profiling,[36] the pattern of gene expression of different liver specimens from the same patient was clustered next to each other. Two macroscopic forms of "liver injury" were distinguished.[37,38] The "diffuse" type fits to our hepatocyte-mediated regeneration model, while the "map-like" type to the one with focus formation. These results suggest that one of the regeneration patterns is at least dominant throughout in the same liver.

The extent of necrosis might be a candidate to reflect the severity of hepatic damage, which determines the form of regeneration.[20,39] Unfortunately, it is very difficult to judge this parameter unequivocally, especially if only one time point is available. Thus, it is not surprising that the related studies provided contradictory results.[8,11,12,40,41]

Three out of our six cases in group 2 had autoimmune hepatitis, while no such etiology occurred in any other groups. Correlation between elevated serum level of AFP and autoimmune hepatitis-caused MHN and elevated serum level of AFP and better prognosis was found in previous studies.[28,29,42] Hepatocyte proliferation has been reported as favorable, while ductular proliferation and the formation of "regenerative nodules" as unfavorable prognostic markers in MHN.[8,11,12] After all, it is not known what determines the form of regeneration: merely the extent or the extent and type of hepatic damage. Nevertheless, the AFP-expressing hepatocytes can be regarded as performers of an efficient liver regeneration, and their presence seems to be a favorable prognostic marker in MHN.

In conclusion, we propose that two forms of liver regeneration can be distinguished in human livers following MHN. If the hepatocytes are able to "dedifferentiate" transiently into AFP expressing, proliferating acinar hepatocytes, they can regenerate the liver. When the hepatocytes fail, the progenitor cells under the influence of portal blood can re-establish the hepatic lobules through the formation of hepatocytic foci. Indirect evidence indicates that this latter form of regeneration is less efficient. Unfortunately, the morphological confirmation of liver regeneration through sequential liver biopsies is not feasible. Thus, the identification of biomarkers (e.g. the dynamic monitoring of serum AFP and/or glypican-3 levels) predicting the probability of native liver recovery may lead to the appearance of novel therapies supporting liver regeneration.

References

1 Weng HL, Cai X, Yuan X *et al*. Two sides of one coin: massive hepatic necrosis and progenitor cell-mediated regeneration in acute liver failure. *Front. Physiol.* 2015; **6**: 1–11.
2 Neuberger J. Prediction of survival for patients with fulminant hepatic failure. *Hepatology* 2005; **41**: 19–21.
3 Lucké B. The pathology of fatal epidemic hepatitis. *Am. J. Pathol.* 1944; **20**: 471–593.
4 Lucké B, Mallory T. The fulminant form of epidemic hepatitis. *Am. J. Pathol.* 1946; **22**: 867–945.
5 Gerber MA, Thung SN, Shen S, Stromeyer FW, Ishak KG. Phenotypic characterization of hepatic proliferation. Antigenic expression by proliferating epithelial cells in fetal liver, massive hepatic necrosis, and nodular transformation of the liver. *Am. J. Pathol.* 1983; **110**: 70–4.
6 Rubin EM, Martin AA, Thung SN, Gerber MA. Morhometric and immunohistochemical characterization of human liver regeneration. *Am. J. Pathol.* 1995; **147**: 397–404.
7 Demetris AJ, Seaberg EC, Wennerberg A, Ionellie J, Michalopoulos G. Ductular reaction after submassive necrosis in humans. Special

emphasis on analysis of ductular hepatocytes. *Am. J. Pathol.* 1996; **149**: 439–48.
8 Chenard-Neu MP, Boudjema K, Bernuau J *et al*. Auxiliary liver transplantation: regeneration of the native liver and outcome in 30 patients with fulminant hepatic failure—a multicenter European study. *Hepatology* 1996; **23**: 1119–27.
9 Fiel MI, Antonio LB, Nalesnik MA, Thung SN, Gerber MA. Characterization of ductular hepatocytes in primary liver allograft failure. *Mod. Pathol.* 1997; **10**: 348–53.
10 Fujita M, Furukawa H, Hattori M, Todo S, Ishida Y, Nagashima K. Sequential observation of liver cell regeneration after massive hepatic necrosis in auxiliary partial orthotopic liver transplantation. *Mod. Pathol.* 2003; **13**: 152–7.
11 Katoonizadeh A, Nevens F, Verslype C, Pirenne J, Roskams T. Liver regeneration in acute severe liver impairment: a clinicopathological correlation study. *Liver Int.* 2006; **26**: 1225–33.
12 Rastogi A, Kumar A, Sakhuja P *et al*. Liver histology as predictor of outcome in patients with acute-on-chronic liver failure (ACLF). *Virchows Arch.* 2011; **459**: 121–7.
13 Hattoum A, Rubin E, Orr A, Michalopoulos GK. Expression of hepatocyte epidermal growth factor receptor, FAS and glypican 3 in EpCAM-positive regenerative clusters of hepatocytes, cholangiocytes, and progenitor cells in human liver failure. *Hum. Pathol.* 2013; **44**: 743–9.
14 Hakoda T, Yamamoto K, Terada R *et al*. A crucial role of hepatocyte nuclear factor-4 expression in the differentiation of human ductular hepatocytes. *Lab. Invest.* 2003; **83**: 1395–402.
15 Stravitz AT, Lefkowitz JH, Fontana RJ *et al*. Autoimmune acute liver failure: proposed clinical and histological criteria. *Hepatology* 2011; **53**: 517–26.
16 Kim H, Park YN. Massive hepatic necrosis with large regenerative nodules. *Korean J. Hepatol.* 2010; **16**: 334–7.
17 Papp V, Dezső K, László V, Nagy P, Paku S. Architectural changes during regenerative and ontogenic liver growth in the rat. *Liver Transpl.* 2009; **15**: 177–83.
18 Dezső K, Papp V, Bugyik E *et al*. Structural analysis of oval-cell-mediated liver regeneration in rats. *Hepatology* 2012; **56**: 1457–67.
19 Dezső K, Rókusz A, Bugyik E *et al*. Human liver regeneration in advanced cirrhosis is organized by the portal tree. *J. Hepatol.* 2017; **66**: 778–86.
20 Itoh T. Stem/progenitor cells in liver regeneration. *Hepatology* 2016; **64**: 663–8.
21 Michalopoulos GK. Liver regeneration. *J. Cell. Physiol.* 2007; **213**: 286–300.
22 Kholodenko IV, Yarygin KN. Cellular mechanisms of liver regeneration and cell-based therapies of liver diseases. *Biomed. Res. Int.* 2017: 8910821.
23 Stueck AE, Wanless IR. Hepatocyte buds derived from progenitor cells repopulate regions of parenchymal extinction in human cirrhosis. *Hepatology* 2015; **61**: 1696–707.
24 Lu W, Bird TG, Boulter L *et al*. Hepatic progenitor cells of biliary origin with liver repopulation capacity. *Nat. Cell Biol.* 2015; **17**: 971–80.
25 Yoon SM, Gerasimidou D, Kuwahara R *et al*. Epithelial cell adhesion molecule (EpCAM) marks hepatocytes newly derived from stem/progenitor cells in humans. *Hepatology* 2011; **53**: 964–73.
26 Taketa K. α-fetoprotein: reevaluation in hepatology. *Hepatology* 1990; **12**: 1420–32.
27 Sell S. Distribution of α-fetoprotein- and albumin-containing cells in the livers of Fischer rats fed four cycles on *N*-2-fluorenylacetamide in a choline-deficient diet. *Am. J. Pathol.* 1984; **114**: 289–300.
28 Schiodt FV, Ostapowitz G, Murray N *et al*. Alpha-fetoprotein and prognosis in acute liver failure. *Liver Transpl.* 2006; **12**: 1776–81.
29 Du W, Pan XP, Li LJ. Prognostic models for acute liver failure. *Hepatobiliary Pancreat. Dis. Int.* 2010; **9**: 122–8.
30 Turányi E, Dezső K, Csomor J, Zs S, Paku S, Nagy P. Immunohistochemical classification of ductular reactions in human liver. *Histopathology* 2010; **57**: 607–14.
31 Hsia CC, Evarts RP, Nakatsukasa H, Marsden ER, Thorgeirsson SS. Occurrence of oval-type cells in hepatitis B virus-associated human hepatocarcinogenesis. *Hepatology* 1992; **16**: 1327–33.
32 Dezső K, Halász J, Bisgaard HC *et al*. Delta-like protein (DLK) is a novel immunohistochemical marker for human hepatoblastomas. *Virchows Arch.* 2008; **452**: 443–8.
33 Ligato S, Mandich D, Cartun RW. Utility of glypican-3 in differentiating hepatocellular carcinoma from other primary and metastatic lesions in FNA of the liver: an immunocytochemical study. *Mod. Pathol.*; **21**: 626–31.
34 Fyfe B, Zaldana F, Liu C. Pathology of acute liver failure. *Clin. Liver Dis.* 2018; **22**: 257–68.
35 Starzl TE, Halgrimson CG, Francavilla FR, Brown TH. The origin, hormonal nature, and action of hepatotrophic substances in portal venous blood. *Surg. Gynecol. Obstet.* 1973; **137**: 179–99.
36 Nissim O, Melis M, Diaz G *et al*. Liver regeneration signature in hepatitis B virus (HBV)-associated acute liver failure identified by gene expression profiling. *PLoS ONE* 2012; **7**: e49611.
37 Koukoulis G, Rayner A, Tan K, Williams R, Portmann B. Immunolocalization of regenerating cells after submassive liver necrosis using PCNA staining. *J. Pathol.* 1992; **166**: 359–68.
38 Quaglia A, Portmann BC, Knisely AS *et al*. Auxiliary transplantation for acute liver failure: histopathological study of native liver regeneration. *Liver Transpl.* 2008; **14**: 1437–48.
39 Das P, Jain D, Das A. A retrospective autopsy study of histopathologic spectrum and etiologic trend of fulminant hepatic failure from North India. *Diagn. Pathol.* 2007; **2**: 27.
40 Hanau C, Munoz SJ, Rubin R. Histopathological heterogeneity in fulminant hepatic failure. *Hepatology* 1995; **21**: 345–51.
41 Li H, Xia Q, Zeng B *et al*. Submassive hepatic necrosis distinguishes HBV-associated acute on chronic liver failure from cirrhotic patients with acute decompensation. *J. Hepatol.* 2015; **63**: 50–9.
42 Yang SS, Cheng KS, Lai YC, Wu CH, Chen TK, Lee CL. Decreasing serum alpha-fetoprotein levels is predicting poor prognosis of acute hepatic failure in patients with chronic hepatitis B. *J. Gastroenterol.* 2002; **37**: 626–32.

Supporting information

Additional supporting information may be found online in the Supporting Information section at the end of the article.

Table S1: Clinical data of the patients.
Table S2: Relationship of the nodules to the portal and arterial and bile duct system.
Table S3: Primary antibodies and fluorescent secondary antibodies used for the immunohistochemical studies.
Figure S1. Connective tissue distribution in Group 1 and Group 3 livers.
Figure S2. Blood supply of ductular reaction in Group 3 livers.
Figure S3. The architecture of the foci.
Figure S4. The architecture of the fused foci.
Figure S5. Regenerating liver lobule.

Movie S1. Localization of a focus in relation to the ductular reaction and portal vein branch.